# A Nonequilibrium Model for Dynamic Simulation of Tray Distillation Columns

**Hendrik A. Kooijman and Ross Taylor**
Dept. of Chemical Engineering, Clarkson University, Potsdam, NY 13699

*A nonequilibrium model for the dynamic simulation of distillation columns is described. The nonequilibrium model includes the direct calculation of the rates of mass and energy transfer and is better able to model the actual physical processes occurring on a real distillation tray than is the conventional equilibrium stage model. Example calculations show that heat-transfer limitations and the vapor holdup above the froth cannot be neglected at elevated pressures. Back-computed Murphree tray efficiencies are not constant over time, which implies that the equilibrium model should not be used for dynamic simulations.*

## Introduction

There are many applications for dynamic simulation of chemical processes. It can be used in the evaluation of process control issues such as design of process control strategy, controller tuning, and testing for intrinsic process controllability. Dynamic simulation can also play a role in process safety assessments and can provide insight into the sizing of equipment and on the flowsheet design; for example, in the validation of the design of heat integrated systems or the design of batch processes for flexible production. Simulation of startup and (automatic emergency) shutdown procedures are used to gain prestartup knowledge.

The simulation of separation processes—in particular the simulation of distillation columns—is an essential part of dynamic process simulators. Distillation is a high energy consumer in most chemical processes, and the interactions between columns can be significant from the design as well as the operability point of view. Early computer models and experiments that appeared in the literature were reported by Mah et al. (1962), Huckaba et al. (1963, 1965), Luyben et al. (1964), Waggoner and Holland (1965), Distefano (1968), and Howard (1970). Usually constant molar holdup was assumed and derivative terms in the energy equation were eliminated. Boston and Britt (1981) developed a commercial batch distillation simulator, based mainly on the model of Distefano. Gallun and Holland (1982) used Gear's method (1971a, b) to solve the equations involved in dynamic simulation. Holland and Liapis (1983) discuss the use of semi-implicit Runge–Kutta methods as well as the multistep methods of Gear for the integration. Prokopakis and Seider (1983) simulated azeotropic distillation towers. Gani et al. (1986, 1987a, b, 1989) and Ruiz et al. (1988) proposed an extended model for the continuous dynamic simulation of distillation columns. The model neglects vapor holdups and uses Murphree plate efficiencies. They used an ODE-solver with a procedural approach for the algebraic constraints and computed Jacobian information by means of finite differencing. Their model is one of the most comprehensive dynamic equilibrium models described in the literature. They also discussed the optimization of the dynamic startup/shutdown operations (Gani et al., 1987a,b) and the hydraulics involved (flooding, entrainment, and weeping). They found that plate hydraulics play an important role in these kinds of simulations. Cuille and Reklaitis (1986) simulated batch distillation with chemical reactions present. Holl et al. (1988) developed a dynamic process simulator called DIVA. Pantelides (1988) included dynamic simulation in the process simulator SPEEDUP. Ranzi et al. (1988) discussed the effects of the energy balances and the way they affect the simulation. They found that the energy balances must be evaluated properly in order to predict correct behavior. Gani and Cameron (1989) proposed the use of a general simulator for steady state as well as dynamic column simulation.

Although the equilibrium model has been the basis of the dynamic simulation of distillation columns, its shortcomings are well known. The model is based on the assumption that both phases leaving a stage are in thermodynamic equilibrium; in practice this never happens. To correct this problem, stage efficiencies are used. For a binary system both compo-

nent efficiencies are equal, but unfortunately this is not the case in systems with more than two components. For ideal and moderately ideal systems the component efficiencies are only a weak function of the composition, in contrast with nonideal systems where the opposite is true. Consequently, in the distillation of nonideal systems the concentration transients could cause large component efficiency changes that might significantly alter the simulation. Component efficiencies are also difficult to calculate (correctly!), and vary over a range from $-\infty$ to $+\infty$. Therefore, efficiencies are often obtained from empirical correlations and assumed equal for all the components, and only dependent on the system of components at hand. In most dynamic simulators efficiencies are held constant, even for nonideal systems where the composition transients imply changes in the component efficiencies over time.

Another assumption of the equilibrium model, thermal equilibrium, forces the liquid and vapor leaving a stage to have the same temperature. In reality, heat transfer between the two phases is limited and the separate phases have their own temperatures. The assumption of thermal equilibrium makes it difficult to model the dynamics of sections in a column that is purposely used for heat transfer.

To eliminate the problems just discussed we need to construct a new dynamic column model that does not employ overall thermodynamic and thermal equilibrium assumptions! A nonequilibrium model was developed by Krishnamurthy and Taylor (1985a–d, 1986) (see, also, Sivasubramanian et al., 1987; Powers et al., 1988; Lao et al., 1989) for steady-state simulation of separation processes. A second-generation model was developed by Taylor et al. (1994) that incorporated the pressure as a variable and eliminated the need for a column design beforehand. This was done by including a design mode that simultaneously computes and adapts the column design during the simulation. Sizing and tray layout are done automatically, and only the type of tray or packing needs to be specified. Taylor et al. (1992) have demonstrated application of the nonequilibrium model to industrial column operations. Since the nonequilibrium model avoids the use of tray efficiencies, it is suitable as a basis for developing a dynamic column model. This article describes such a model for tray columns.

## Model Assumptions

A diagram of a general tray in a column is provided in Figure 1. Of central importance is the zone where vapor and liquid phases are brought into contact with each other in order to promote mass and energy transfer between the phases. A tray can operate in different flow regimes: spray, froth, emulsion, bubbling liquid, or foam. Here we will generally refer to the dispersion on the tray as the froth, although we do not limit our model to that regime. Above the froth is an area for vapor disengagement, to separate the phases to let them move countercurrently in the column. Similarly, we have a downcomer for liquid disengagement. These disengagement areas are essential to the operation of a trayed column and certainly play a role in its performance.

What differentiates the dynamic model from the steady-state model (as described by Taylor et al., 1994) is the use of holdup terms. For steady-state simulation, holdup calculations are not required; however, in the dynamic model they represent the basic differential equations. For the general tray, a number of distinct holdups can be identified:

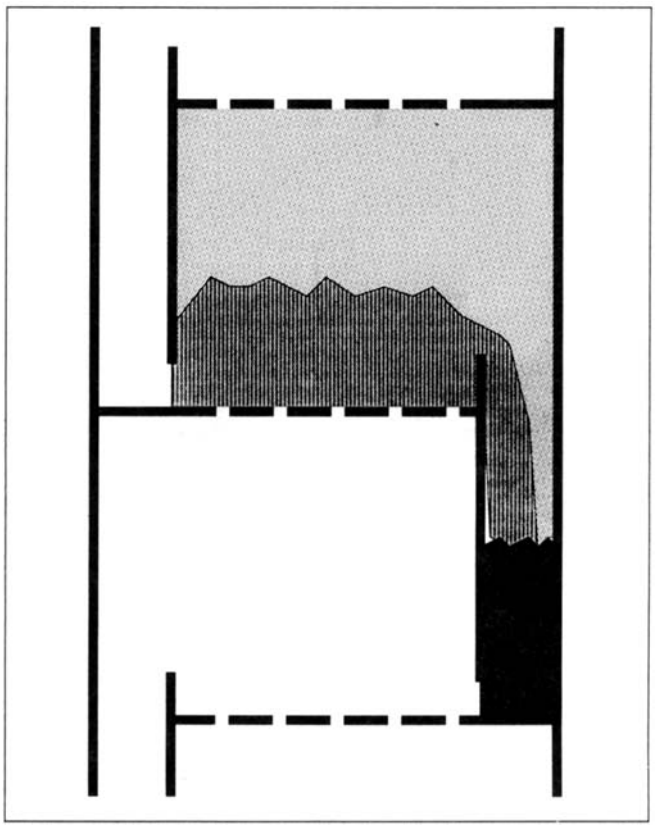

**Figure 1. General tray.**

- Liquid in the froth on a tray
- Vapor dispersed in the froth on a tray
- Liquid in the downcomer below a tray
- Vapor above the froth/downcomer on a tray.

The froth is modeled by two (or more, if multiple liquid phases are present) separate holdups. Figure 2 is a diagram of these holdups and also shows the connecting flows between the different holdups. The following assumptions have been made in our dynamic nonequilibrium model:

- The trays are in mechanical equilibrium.
- Thermodynamic equilibrium is assumed *only* at the interface between vapor and liquid phases on the tray.
- Mass transfer occurs *only* between vapor and liquid on the tray, dictated by the resistance to transport in each phase.
- Condenser and reboiler operate at equilibrium (due to their design).

The dynamic model developed here uses all four holdup terms and avoids simplifications often made in other dynamic models, such as constant holdups, neglecting energy derivatives, neglecting vapor holdups, and constant (tray/component) efficiencies. To reduce the size of the model, the holdup terms for the vapor above the froth and in the downcomer can be lumped into the froth holdups (if it is desired to do so).

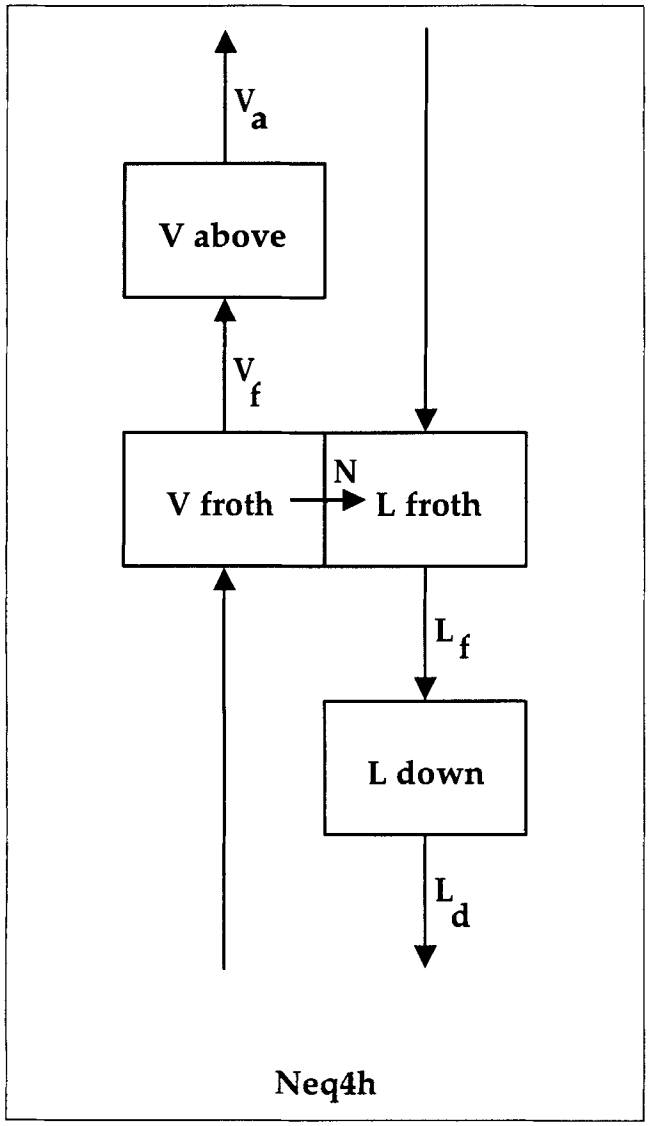


**Figure 2. Holdups and connecting flows.**

## Model Equations

Component molar holdup terms are denoted with $U_{ij}^{Pw}$, where $P$ indicates the holdup phase type ($V$ or $L$), $w$ the place in the model ($f$ for froth, $d$ for downcomer, and $a$ for above the froth), $i$ the component, and $j$ the plate number. Similarly, total molar holdups are denoted with $U_{tj}^{Pw}$ and energy holdups with $E_j^{Pw}$. Vapor and liquid holdup compositions are computed from

$$y_{ij}^{w} = \frac{U_{ij}^{Vw}}{U_{tj}^{Vw}} \tag{1}$$

$$x_{ij}^{w} = \frac{U_{ij}^{Lw}}{U_{tj}^{Lw}}. \tag{2}$$

The interstage liquid and vapor flows on plate $j$ are denoted with $L_j^w$ and $V_j^w$, where $w$ indicates the holdup from which the flows originate ($f$, $d$, or $a$). Component molar feed flows are denoted similarly to molar holdups as $F_{ij}^{Pw}$. The mass-transfer rates through the interface are positive from vapor to liquid and denoted by $N_{ij}^{w}$.

For a general stage (one not at the top or bottom of the column) the component molar balances over the four different holdups are:

$$\frac{dU_{ij}^{Vf}}{dt} = y_{i,j+1}^{a} V_{j+1}^{a} + F_{ij}^{Vf} - y_{ij}^{f} V_j^f - N_{ij}^{f} \tag{3}$$

$$\frac{dU_{ij}^{Lf}}{dt} = x_{i,j-1}^{d} L_{j-1}^{d} + F_{ij}^{Lf} - x_{ij}^{f} L_j^f + N_{ij}^{f} \tag{4}$$

$$\frac{dU_{ij}^{Va}}{dt} = y_{ij}^{f} V_j^f + F_{ij}^{Va} - y_{ij}^{a} V_j^a \tag{5}$$

$$\frac{dU_{ij}^{Ld}}{dt} = x_{ij}^{f} L_j^f + F_{ij}^{Ld} - x_{ij}^{d} L_j^d. \tag{6}$$

These equations may be extended to include fractional entrainment ($\Phi_j^L$, $\Phi_j^V$), weep flow ratios ($w_j$), sidestream flow ratios ($r_j$), and interlinking flows ($G_{ijv}$). This is not done here (see, however, Taylor et al., 1994). To correctly model the behavior of a column outside normal operational conditions, inclusion of entrainment and weep flows is essential.

The component molar holdups must sum to the total molar holdups:

$$0 = \sum_{i=1}^{c} U_{ij}^{Vf} - U_{tj}^{Vf} \tag{7}$$

$$0 = \sum_{i=1}^{c} U_{ij}^{Lf} - U_{tj}^{Lf} \tag{8}$$

$$0 = \sum_{i=1}^{c} U_{ij}^{Va} - U_{tj}^{Va} \tag{9}$$

$$0 = \sum_{i=1}^{c} U_{ij}^{Ld} - U_{tj}^{Ld}. \tag{10}$$

The energy balances for each holdup are:

$$\frac{dE_j^{Vf}}{dt} = \frac{E_{j+1}^{Va}}{U_{t,j+1}^{Va}} V_{j+1}^{a} + \sum_{i=1}^{c} H_{ij}^{FVf} F_{ij}^{Vf} - \frac{E_j^{Vf}}{U_{tj}^{Vf}} V_j^f - \epsilon_j^{Vf} + Q_j^{Vf} \tag{11}$$

$$\frac{dE_j^{Lf}}{dt} = \frac{E_{j-1}^{Ld}}{U_{t,j-1}^{Ld}} L_{j-1}^{d} + \sum_{i=1}^{c} H_{ij}^{FLf} F_{ij}^{Lf} - \frac{E_j^{Lf}}{U_{tj}^{Lf}} L_j^f + \epsilon_j^{Lf} + Q_j^{Lf} \tag{12}$$

$$\frac{dE_j^{Va}}{dt} = \frac{E_j^{Vf}}{U_{tj}^{Vf}} V_j^f + \sum_{i=1}^{c} H_{ij}^{FVa} F_{ij}^{Va} - \frac{E_j^{Va}}{U_{tj}^{Va}} V_j^a + Q_j^{Va} \tag{13}$$

$$\frac{dE_j^{Ld}}{dt} = \frac{E_j^{Lf}}{U_{tj}^{Lf}} L_j^f + \sum_{i=1}^{c} H_{ij}^{FLd} F_{ij}^{Ld} - \frac{E_j^{Ld}}{U_{tj}^{Ld}} L_j^d + Q_j^{Ld}, \tag{14}$$

where $\epsilon$ is the energy transport to/from the interface (see below), $H_{ij}^{FPw}$ is the partial molar enthalpy of component $i$ in

the feed to the specified holdup, and $Q_j^{Pw}$ is the heat input into the specified holdup. The energy holdups $E_j^{Pw}$ are related to the component molar holdups and the component enthalpies ($H_{ij}^{Pw}$) by

$$0 = \sum_{i=1}^{c} \left(H_{ij}^{Vf} U_{ij}^{Vf}\right) - E_j^{Vf} \tag{15}$$

$$0 = \sum_{i=1}^{c} \left(H_{ij}^{Lf} U_{ij}^{Lf}\right) - E_j^{Lf} \tag{16}$$

$$0 = \sum_{i=1}^{c} \left(H_{ij}^{Va} U_{ij}^{Va}\right) - E_j^{Va} \tag{17}$$

$$0 = \sum_{i=1}^{c} \left(H_{ij}^{Ld} U_{ij}^{Ld}\right) - E_j^{Ld}. \tag{18}$$

Enthalpies are functions of the holdup temperature, $T_j^{Pw}$, pressure, $P_j$, and holdup molar compositions. The energy fluxes from the vapor to the interface and from the interface to the liquid on plate $j$ are

$$\epsilon_j^{Vf} = \sum_{i=1}^{c} N_{ij}^{Vf} H_{ij}^{Vf} + h_j^{Vf} a_j \left(T_j^{Vf} - T_j^{I}\right) \tag{19}$$

$$\epsilon_j^{Lf} = \sum_{i=1}^{c} N_{ij}^{Lf} H_{ij}^{Lf} + h_j^{Lf} a_j \left(T_j^{I} - T_j^{Lf}\right), \tag{20}$$

where $T_j^I$ is the temperature of the interface on plate $j$. The energy balance over the interface equates these energy fluxes:

$$0 = \epsilon_j^{Vf} - \epsilon_j^{Lf}. \tag{21}$$

The interface compositions $x_{ij}^{If}$ and $y_{ij}^{If}$ must sum to unity,

$$0 = \sum_{i=1}^{c} y_{ij}^{If} - 1 \tag{22}$$

$$0 = \sum_{i=1}^{c} x_{ij}^{If} - 1 \tag{23}$$

and obey the equilibrium relations ($i = 1 \ldots c$) as well:

$$0 = K_{ij}^{If} x_{ij}^{If} - y_{ij}^{If}. \tag{24}$$

The mass-transfer rates $N_{ij}$ from the vapor to the interface are equal to the mass-transfer rates from the interface to the liquid. They are computed with the following rate equations:

$$(0) = (N_j) - N_{tj}\left(y_j^{Vf}\right) - c_j^{Vf} a_j \left[R_j^{Vf}\right]^{-1} \left[\Gamma_j^{Vf}\right] \left(\left(y_j^{Vf}\right) - \left(y_j^{If}\right)\right) \tag{25}$$

$$(0) = (N_j) - N_{tj}\left(x_j^{Lf}\right) - c_j^{Lf} a_j \left[R_j^{Lf}\right]^{-1} \left[\Gamma_j^{Lf}\right] \left(\left(x_j^{If}\right) - \left(x_j^{Lf}\right)\right), \tag{26}$$

where $N_{tj}$ is the total mass-transfer rate on plate $j$, which equals the sum of all the component mass-transfer rates $N_{ij}$. Note that only $c-1$ fluxes are independent, and we will obtain $2(c-1)$ equations. Also note that the rate equations are in matrix/vector form.

The rate matrix $[R]$ ($c-1$ by $c-1$) is calculated from binary mass-transfer coefficients:

$$R_{ii} = \frac{x_i}{k_{ic}} + \sum_{m=1, m \neq i}^{c} \frac{x_m}{k_{im}} \tag{27}$$

$$R_{ij} = -x_i \left(\frac{1}{k_{ij}} - \frac{1}{k_{ic}}\right) \quad i \neq j. \tag{28}$$

For systems where an activity coefficient model is used for the phase equilibrium properties, the thermodynamic factor matrix $\Gamma$ (order $c-1$) is defined by

$$\Gamma_{ij} = \delta_{ij} + x_i \left(\frac{\partial \ln \gamma_i}{\partial x_j}\right)_{T,P,x_k, k \neq j = 1 \ldots n-1} \tag{29}$$

If an equation of state is used, $\gamma_i$ is replaced by $\phi_i$. Expressions for the composition derivatives of $\ln \gamma_i$ are given by Taylor and Kooijman (1991).

Pressure $P_j$ is computed from the tray pressure drop and pressure of the tray above. The pressure at the top of the column is specified ($P_{\text{spec}}$):

$$0 = p_1 - P_{\text{spec}} \tag{30}$$

$$0 = p_j - p_{j-1} - \Delta P_{j-1}, \tag{31}$$

where $\Delta P_{j-1}$ is the pressure drop for the specific type of column internals (computed empirically or theoretically, Taylor et al., 1994).

The interholdup flow rates are determined through calculation of the total molar holdups (alternatively, they could be computed directly from empirical or theoretical relations). The total molar holdups can be computed from the height of the froth, $h_j^f$, the clear liquid height, $h_j^{cl}$, the tray spacing, $h_j^{ts}$, and the liquid height in the downcomer, $h_j^d$, of plate $j$:

$$0 = \left(h_j^f - h_j^{cl}\right) A_j^f c_j^{Vf} - U_{tj}^{Vf} \tag{32}$$

$$0 = h_j^{cl} A_j^f c_j^{Lf} - U_{tj}^{Lf} \tag{33}$$

$$0 = \left\{\left(h_j^{ts} - h_j^f\right) A_j^b + \left(2h_j^{ts} - h_j^d\right) A_j^d\right\} c_j^{Va} - U_{tj}^{Va} \tag{34}$$

$$0 = h_j^d A_j^d c_j^{Ld} - U_{tj}^{Ld}. \tag{35}$$

The liquid heights are computed by empirical correlations or theoretical relations. Note that each total holdup must be a function of the relevant flow rate (such as $U_{tj}^{Ld}$ should be a function of $L_j^d$) to prevent higher index systems. Since this is not the case for Eq. 34, we can replace it with

$$0 = V_j^f - V_j^a \tag{36}$$

to use a constant molar vapor holdup above the froth (usually the change in $U_{tj}^{Va}$ is small). This assumption maintains the

index of the system at one (instead of two), but violates the physical constraint of a fixed volume between the trays. For the correct dynamic simulation, it is important that the liquid height correlations behave correctly besides being accurate (which is not required for steady-state simulation).

The total number of equations is $7c+18$ per general stage, where $c$ represents the number of components in the system. Out of these, $4c+4$ equations are ordinary differential equations, while the rest $(3c+14)$ are algebraic equations. The feed flows ($F$), heat inputs ($Q$), top and condenser pressures ($P_{\text{spec}}$, $P^c$), and product streams ($D$, $B$) are functions of time. If they are constants, we are solving a steady-state (SS) process, where all differential terms are set to zero. If they change over time, we switch to dynamic simulation (DS), where we solve the resulting differential–algebraic system of equations until steady state is reached (or until the variable changes are less than some specified small fraction). Of course, only during a SS simulation can we activate the *design mode*, which simultaneously corrects the column design to handle the process flows at hand. The resulting design can then be directly used for the dynamic simulation.

A simplification of this full tray model results from ignoring the vapor above the froth and the liquid in the downcomer. Equations 5, 6, 9, 10, 13, 14, 17, 18, 34 and 35 are omitted from this model, which has just $5c+10$ variables. The neglected downcomer and vapor holdup could be optionally lumped into the liquid and vapor holdup equations (Eqs. 32 and 33).

Distillation columns also have various types of condensers and reboilers that usually have a significantly larger holdup than the holdup on any tray. It is these larger holdups that lead to differences in the transient behavior of various variables, and therefore have a large effect on the column behavior. They also cause the system of equations to be very stiff.

The reboiler is modeled as a liquid holdup in the bottom of the column followed by a partial (equilibrium) reboiler. The holdup component molar balances ($c$) are

$$\frac{dU_{ib}^L}{dt} = x_{in}L_n^d - x_{ib}L_b, \tag{37}$$

where the liquid mole fraction is $x_{ib} = U_{ib}^L/U_{tb}^L$ and the tray above the reboiler is tray $n$. The total holdup is computed by summing the component holdups:

$$0 = \sum_{i=1}^{c} U_{ib}^L - U_{tb}^L. \tag{38}$$

Assuming a constant molar holdup, we write the total molar balance (for dynamic state):

$$0 = L_n^d - L_b. \tag{39}$$

For steady state this equation is replaced by a direct specification of the molar (or possibly volumetric) holdup in the reboiler:

$$0 = U_{tb}^L - U_{tb,\text{spec}}^L. \tag{40}$$

The energy holdup and energy relation are

$$\frac{dE_b}{dt} = \frac{E_n^{Ld}}{U_n^{Ld}}L_n^d - \frac{E_b}{U_{tb}^L}L_b \tag{41}$$

$$0 = \sum_{i=1}^{c} (H_{ib}^L U_{ib}^L) - E_b. \tag{42}$$

The pressure is determined from

$$0 = p_b - p_n - \Delta P_n. \tag{43}$$

For a partial reboiler we have total and component molar balances $(c+1)$, equilibrium relations ($c$), a summation equation for the vapor and liquid mole fractions (1), and an energy balance (1):

$$0 = L_b - V_r - B \tag{44}$$

$$0 = x_{ib}L_b - y_{ir}V_r - x_{ir}B \tag{45}$$

$$0 = K_{ir}x_{ir} - y_{ir} \tag{46}$$

$$0 = \sum_{i=1}^{c} (y_{ir} - x_{ir}) \tag{47}$$

$$0 = \frac{E_b}{U_{tb}^L}L_b + Q_r - H_r^V V_r - H_r^L B \tag{48}$$

where $Q_r$ represents the reboiler duty, $B$ the bottoms flow, and $V_r$ the boilup vapor returned to stage $n$. Various reboiler specifications can be used, for example, the specification of the bottoms flow:

$$0 = B - B_{\text{spec}}. \tag{49}$$

The $(3c+9)$ variables are $U_{ib}^L$, $U_{tb}^L$, $E_b$, $T_b$, $L_b$, $P_b$, $V_r$, $y_{ir}$, $Q_r$, $T_r$, $x_{ir}$, and $B$. In the case of a total reboiler with a *vapor* product, $x_{ir}B$ in the reboiler mole balance becomes $y_{ir}B$ and $H_r^L B$ in the energy balance becomes $H_r^V B$. For a total reboiler with a *liquid* product, $x_{ir}B$ in the reboiler mole balance becomes $x_{ib}B$ and $H_r^L B$ in the energy balance becomes $E_b B/U_{tb}^L$.

The condenser is modeled as a total condenser and reflux drum. The total condenser has the normal $(2c+3)$ equations. The variables are the liquid product flow, $L_c$, the temperature, $T_c$, heat duty, $Q_c$, and the vapor and liquid mole fractions, $x_{ic}$ and $y_{ic}$. The condenser equations are, respectively, a total molar balance, component molar balances ($c$), an energy balance, equilibrium relations ($c$), and a summation equation:

$$0 = V_2 - L_c \tag{50}$$

$$0 = y_{i2}V_2 - x_{ci}L_c \tag{51}$$

$$0 = H_2^V V_2 + Q_c - H_c^L L_c \tag{52}$$

$$0 = K_{ic}x_{ic} - y_{ic} \tag{53}$$

$$0 = \sum_{i=1}^{c} (y_{ic} - x_{ic}). \tag{54}$$

The pressure of the condenser, $P_{cond}$, is specified. The reflux drum has a vapor and a liquid holdup. Thus, we have $c$ component molar holdups ($U_i^{L\text{drum}}$), a total molar holdup ($U_t^{L\text{drum}}$), and an energy holdup ($E^{L\text{drum}}$). We have a liquid distillate flow ($D^L$) and a returning liquid reflux ($R$). The molar component holdup, total holdup and energy balances are:

$$\frac{dU_i^{L\text{drum}}}{dt} = x_{ic}L_c - x_i^{\text{drum}}(D^L + R) \tag{55}$$

$$0 = \sum_{i=1}^{c} U_i^{L\text{drum}} - U_t^{L\text{drum}} \tag{56}$$

$$\frac{dE^{L\text{drum}}}{dt} = H_c^L L_c - \frac{E^{L\text{drum}}}{U_t^{L\text{drum}}}(D^L + R). \tag{57}$$

The energy holdups are equated to the products of the molar holdups and enthalpies to determine the liquid drum temperature ($T^{L\text{drum}}$):

$$0 = \sum_{i=1}^{c} (U_i^{L\text{drum}} H_i^{L\text{drum}}) - E^{L\text{drum}}. \tag{58}$$

We have a total of $c+5$ equations and variables: $U_i^{L\text{drum}}$, $U_t^{L\text{drum}}$, $E^{L\text{drum}}$, $T^{L\text{drum}}$, $R$, and distillate rate $D^L$. Combined with the condenser, this gives $3c+8$ variables and $3c+6$ equations. The extra equations needed are the condenser specification and constraint. For unsteady-state simulation the condenser constraint is a constant molar (or volume) holdup:

$$0 = L_c - (D^L + R). \tag{59}$$

Again, for the steady-state simulation, this equation is replaced by the direct specification of the molar (or volume) holdup:

$$0 = U_t^{L\text{drum}} - U_{t,\text{spec}}^{L\text{drum}}. \tag{60}$$

Various steady-state condenser specifications can be used. For example, fixing the reflux ratio ($RR$) is represented by

$$0 = D^L RR - R. \tag{61}$$

The $3c+8$ variables and equations of the condenser are $L_c$, $x_{ic}$, $T_c$, $y_{ic}$, $Q_c$, $U_i^{L\text{drum}}$, $E^{L\text{drum}}$, $U_t^{L\text{drum}}$, $T^{L\text{drum}}$, $R$, and $D^L$. The vapor/liquid holdups in the connecting pipes between column and condenser/reboiler are neglected, but can be incorporated if necessary.

To compare results of the nonequilibrium model with those of the conventional equilibrium-based simulations, an equilibrium tray model with a specified tray efficiency, $\xi_j$ (which is constant over the integration interval), is used (Kooijman, 1995). In this model the vapor holdups are neglected and only the liquid holdup in the froth is included. This holdup can be computed by Eq. 33 or held constant (computed at steady state or user specified). The tray pressures are computed with the tray pressure drops (the pressure of the tray at the top of the column specified). We obtain $2c+6$ equations and variables ($U_{ij}$, $U_{tj}$, $E_j$, $y_{ij}$, $V_j$, $L_j$, $T_j$, and $P_j$). If the vapor holdup is not neglected but also computed, we obtain a model with $2c+8$ equations and variables ($U_{ij}^V$, $U_{ij}^L$, $U_{tj}^V$, $U_{tj}^L$, $E_j^V$, $E_j^L$, $V_j$, $L_j$, $T_j$, and $P_j$). Again, neglected holdups could be included as discussed previously.

We have discussed four different models: the nonequilibrium model with four holdup terms (NEQ4H), the nonequilibrium model with only two froth holdup terms (NEQ2H), the equilibrium model with liquid holdup terms (EQL), and the equilibrium model with both liquid and vapor holdup terms (EQLV). With these four models we shall explore the differences between the dynamic nonequilibrium and equilibrium models.

## Physical Property Models

The physical property models that supply the $K$-values, activity coefficients, binary diffusivities, densities, heat capacities, enthalpies, vapor pressures, viscosities, thermal conductivities, surface tensions, and binary mass-transfer coefficients are a large and important part of a process simulator. Mass-transfer coefficients $k_{ij}$, are computed from empirical models (Taylor and Krishna, 1993) and multicomponent diffusion coefficients evaluated from an interpolation formula (Kooijman and Taylor, 1991). A nonequilibrium model has a much higher demand for properties than does an equilibrium model (Taylor et al., 1994). Property models also impose a problem specially associated with dynamic simulation. Often, different correlations are used over different state variable ranges. When a switch between different correlations occurs due to a change in a state variable (such as temperature, pressure, or composition), it causes a discontinuity in the simulation. For the sake of consistency, properties need to be continuous at or around any switching points. Depending on the solver used, proper handling of these discontinuities *may* require the physical property model/correlation switches to be signaled in some way. However, this is not (yet) done in the present implementation of the models described earlier. Rather, discontinuities of this kind are avoided as much as possible by using a single correlation for the whole integration.

## Solving the Model Equations

The system of model equations consists of differential equations for the molar and energy balances and algebraic equations for all other relations; a differential–algebraic (DAE) system. Two methods are used to solve DAE systems. The procedural approach solves the algebraic equations separately from the differential equations. True DAE solvers solve the whole system of equations. There are two main types of such DAE solvers: solvers that employ backwards differentiation formulas (BDF) and one-step (semi-)implicit methods (such as Runge–Kutta methods). The advantage of using one-step methods is that they do not require (consistent) initial derivative information, which is hard to obtain (for the algebraic variables). The approach used here (referred to as BESIRK) consists of a semi-implicit Runge–Kutta method developed originally by Michelsen (1976), but that is extended with an extrapolation technique (Bulirsh and Stoer, 1966) to improve the efficiency in solving DAE problems. One

of the limitations of this implementation is the fact that the differential terms must have constant coefficients. It is for this reason that molar holdups are used as model variables instead of molar compositions.

The models are set up in a specific manner so that we can easily switch between solving a steady state and dynamic problems. This allows us to use the dynamic model as a relaxation method for solving steady-state problems (Gani and Cameron, 1989). A problem is started with a steady-state simulation to initialize all the variables. Then a disturbance can be introduced and the dynamic simulation can start. When, during a dynamic simulation, the variables do not change by more than a predefined fraction (here, $10^{-3}$), a switch to the steady-state simulation is initiated. Care must be taken that the DAE solver is started with a consistent set of initial variables where the algebraic constraints are satisfied (in the case of the nonequilibrium model, this can easily be done by assuming zero interface fluxes and computing molar and energy holdups).

The system of model equations is sparse since each stage is usually only connected with the stage below and the stage above. To exploit this sparsity of the problem and to solve it efficiently we use the NSPIV sparse solver (Sherman, 1978). NSPIV does not save LU factors and cannot exploit the fact that multiple linear systems with the same matrix need to be solved. However, solving the sparse linear systems is isolated in one routine to easily switch to other sparse solvers such as MA28 (Duff, 1979).

To employ a BDF or (semi-)implicit Runge–Kutta method we need the Jacobian of the righthand side of all the equations. This information is computed from analytical expressions with the exception of the enthalpies, heat-transfer coefficients (Eqs. 19 and 20), rate equations (Eqs. 25 and 26), holdup equations (Eqs. 32–35), and pressure drop derivatives (Eq. 31). Obtaining an "analytical" Jacobian is cumbersome, but with a numerically computed Jacobian (by finite differencing) the integration becomes rather slow (even when exploiting the sparsity of the system). Furthermore, the accuracy of the Jacobian can be very important for SIRK methods and in the exact locating of discontinuities. BESIRK retains a copy of the Jacobian in order to save Jacobian evaluations.

The program keeps track of the index of the system of equations. This index indicates the number of times the algebraic constraints have to be differentiated with respect to the independent variable (time) to produce a system of only ordinary differential equations. Higher index problems are usually more difficult to solve. BESIRK can signal warning messages when the index is higher than one (BESIRK tests if the Jacobian matrix of the algebraic equations with respect to the algebraic variables is singular; if so, the index is considered higher than one and Jacobian information is used to obtain an estimate of the index).

The full dynamic nonequilibrium model was implemented on the PC platform in Fortran, running small to moderate dynamic simulation problems on a 66-MHz 486 (with 8-MByte RAM) within several hours. The simulation program uses analytical derivatives to reduce CPU requirements, but was not (yet) optimized for speed or memory requirements. For example, certain (transport) property derivatives might not need to be continuously computed.

## Simulation Results

The results presented here mainly highlight some of the differences between dynamic equilibrium and nonequilibrium models. Four examples have been simulated, an extractive distillation column, an acetone absorber, a debutanizer adapted from Gani et al. (1986), and a depropanizer taken from Taylor et al. (1994). Steady-state results for the nonequilibrium models described earlier are identical to those from the model of Taylor et al. (1994), even though the model equations differ both in form and in number (the latter uses mole fractions since, for steady state, no holdups of any kind need to be computed). Newton's method was used to obtain the steady-state solution. Through the use of exact Jacobians, convergence (in terms of number of iterations) was improved over the steady-state-only implementation (which uses only composition derivatives of the rate equations). The results of the two different dynamic equilibrium models (EQL and EQLV) were very similar. For comparisons the EQLV equilibrium model and the NEQ2H nonequilibrium models were used except where otherwise indicated.

### *Extractive distillation*

Our first example is an extractive distillation column that separates *n*-heptane and toluene using phenol as the extractive agent. Temperature sensors often are used to control this kind of extractive distillation column. Thus, we are interested in the differences in temperature profiles between equilibrium and nonequilibrium simulations of this type of column. The simulated column has 29 sieve plates, a partial reboiler, and a total condenser. The column has a 50/50 mol % feed of toluene and *n*-heptane at stage 20 (counting from the top, including the condenser as the first stage) and a phenol feed at stage 10 that is three-and-a-half times larger than our original feed. The phenol makes the *n*-heptane more volatile than the toluene and the distillate purity is about 98.5 mol %. The tray design was automatically generated by the nonequilibrium model (based on a design of 0.75 fraction of flooding). The same sieve tray design was taken for all the simulations to compare the results for the various models. The AIChE model (Gerster et al., 1958) was used for calculation of the mass-transfer coefficients. The condenser and reboiler holdup were set to account for a liquid holdup of about 5 min (at a reflux ratio of 5). See Table 1 for a summary of the simulations.

To compare the two types of simulation, it is necessary to use a Murphree tray efficiency for the equilibrium model that is a back-calculated average from the nonequilibrium simulation. This is needed to obtain an equilibrium simulation with the same number of trays, and therefore, comparable dynamic behavior. An equilibrium model with constant Murphree efficiency of 55% for all the components gave similar products as those obtained in a nonequilibrium simulation. The computed steady-state component Murphree efficiencies are shown in Figure 3. Notice that the component efficiencies are generally unequal and can vary outside the range from zero to one. Here, the efficiencies change radically and are very different from their average value, especially around the phenol feed. This is due to the fact that the phenol feed is subcooled (by about 40°C) for better separation, but it is still hotter than the internal flows at the feedtray. Therefore,

**Table 1. Extractive Distillation Column Specifications**

| | | | |
|---|---|---|---|
| DECHEMA K model | | | |
| UNIQUAC model (parameters by UNIFAC) | | | |
| Antoine vapor pressure | | | |
| Excess enthalpy | | | |
| Condenser pressure 2.0 (bar) | | | |
| Top pressure 2.0 (bar) | | | |
| Estimated pressure drop | | | |
| Feed stage | | 10 | 20 |
| Vapor fraction | | | 0 |
| Temperature (°C) | | 170 | |
| Component flows (mol/s) | | | |
| *n*-heptane | | 0 | 25 |
| Toluene | | 0 | 25 |
| Phenol | | 175 | 0 |
| Total Condenser (stage 1): | | | |
| Reflux ratio = 5.0 | | | |
| Molar holdup = 45.0 (kmol) | | | |
| Partial Reboiler (stage 31): | | | |
| Bottom product flow rate = 200.0 (mol/s) | | | |
| Molar holdup = 90.0 (kmol) | | | |
| Section | 1 | 2 | 3 |
| First stage | 2 | 10 | 20 |
| Last stage | 9 | 19 | 30 |
| Column dia. (m) | 2.57 | 2.09 | 2.17 |
| Total tray area ($m^2$) | 5.19 | 3.43 | 3.70 |
| No. of flow passes | 3 | 2 | 2 |
| Tray spacing (m) | 0.5 | 0.5 | 0.5 |
| Liquid flow path length (m) | 0.717 | 0.778 | 0.753 |
| Active area (% total) | 86.8 | 82.0 | 77.8 |
| Total hole area (% active) | 12.1 | 9.8 | 9.6 |
| Downcomer area (% total) | 6.6 | 9.0 | 11.1 |
| Hole diameter (m) | 0.00476 | 0.00476 | 0.00476 |
| Hole pitch (m) | 0.0130 | 0.0144 | 0.0144 |
| Weir length (m) | 6.23 | 3.56 | 3.67 |
| Weir height (m) | 0.0508 | 0.0508 | 0.0508 |
| Downcomer clearance (m) | 0.0381 | 0.0381 | 0.0381 |
| Deck thickness (m) | 0.00254 | 0.00254 | 0.00254 |

the nonequilibrium model has a higher liquid temperature on the feed tray than the equilibrium model due to limited heat transfer with the vapor. This phenomenon cannot be observed with the equilibrium model since it requires thermal equilibrium.

The column was perturbed by decreasing the phenol feed temperature from 170 to 140°C. Computed Murphree efficiencies of the steady state after this perturbance are shown in Figure 4. Note the differences with Figure 3. Since the efficiencies change over time, the dynamic results computed with constant efficiencies in the equilibrium model become an approximation to the actual dynamic behavior. The changes in the temperature profiles as a function of time for the equilibrium and nonequilibrium model are shown in Figure 5. There we can observe that the difference between the lines of the equilibrium model (dashed) and the nonequilibrium model (solid) can vary in a nonlinear fashion with time. This implies that the dynamic response for the temperatures on these plates is quantitatively and qualitatively different, with obvious implications for any control strategies derived from the simulations. The temperatures for the nonequilibrium model seem to fluctuate much less than those for the equilibrium model, since mass- and heat-transfer limitations dampen the changes quicker. The fluctuations are due to the sudden increase in a cooler liquid flow going down the column, which will result in extra vapor being condensed below

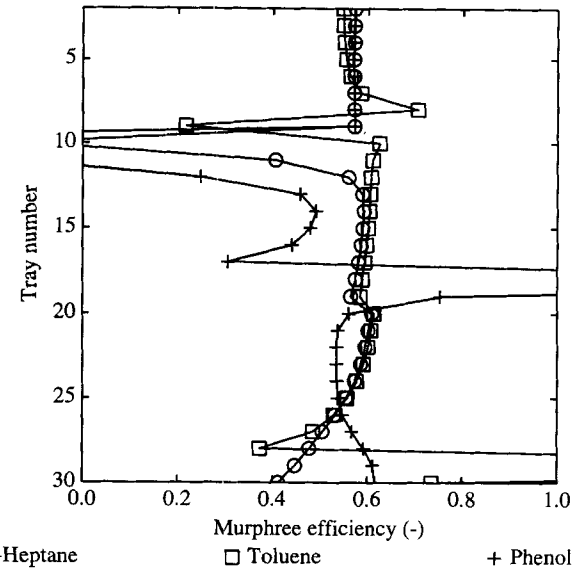


**Figure 3. Murphree efficiencies backcalculated from nonequilibrium simulation for the extractive distillation of *n*-heptane and toluene with phenol.**

the phenol feed. When this extra liquid reaches the reboiler, the vapor flow quickly rises (because the bottoms flow is constant), and so the internal liquid flow decreases. The vapor is condensed and partially returned to the column (since a reflux ratio was specified, and the condenser holdup is constant). This will send another wave of increased liquid flow down the column, but one that is smaller than the original one. For illustration the liquid and vapor flows have been

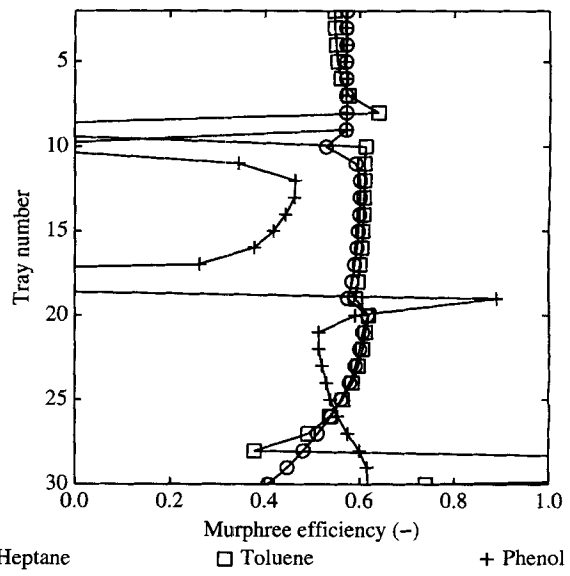


**Figure 4. Murphree efficiencies backcalculated from nonequilibrium simulation for the extractive distillation after a drop in phenol feed temperature.**

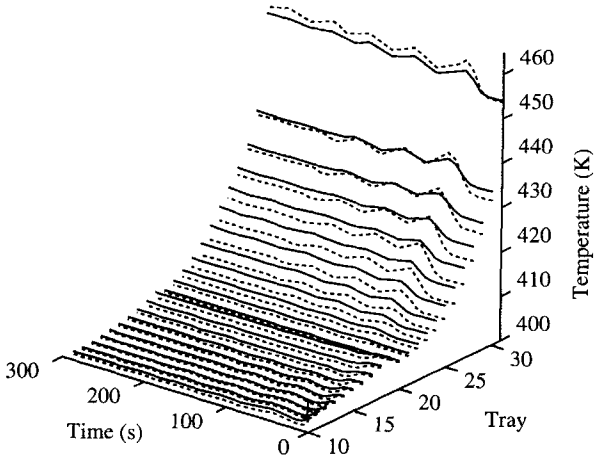


**Figure 5. Temperatures (K) of trays 10 through 30 and the reboiler for the extractive distillation column as a function of time.**

plotted as a function of time in Figures 6 and 7, respectively. Of course, with variable condenser and reboiler holdups the oscillations in the internal flows would be less pronounced or suppressed. But the initial wave of liquid down the column from the feed flow causes a nonlinear response that is quite different for both the models.

### *Acetone absorber*

The second example consists of a 30 sieve tray absorber in which acetone is to be absorbed in water from a vapor stream (specifications are given in Table 2). The column is perturbed by increasing the vapor feed temperature from 25 to 100°C. The column was simulated first with the nonequilibrium model (using the AIChE model for mass-transfer coefficients) in design mode to obtain a suitable sieve-tray design and a back-calculated average Murphree efficiency (of 0.34) for the equilibrium simulation.

Initially the nonequilibrium model temperature profile (Figure 8) shows the typical bulge (of 2 to 3°C) caused by the heat of absorption of acetone in water and the evaporation

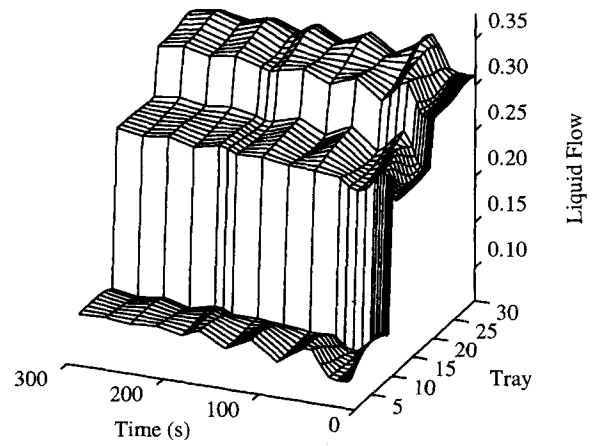


**Figure 6. Internal liquid flows for the extractive distillation column as a function of time.**

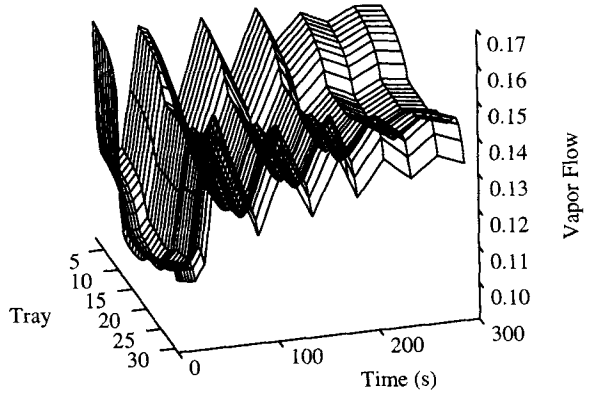


**Figure 7. Internal vapor flows for the extractive distillation column as a function of time.**

of water in the bottom. After the vapor feed temperature increase, the liquid temperatures in the whole column rise as well. The equilibrium model initially predicts a very similar temperature bulge at about the same tray (Figure 9). However, after perturbation we see that the liquid temperature on the bottom tray quickly rises to a higher value than any of the tray above it. This is due to the assumptions that the temperature of the leaving flows on a tray have to be the same. Therefore, the model predicts that the vapor entering the bottom of the column, which has a temperature much higher than that of the liquid, is cooled down to the temperature of the liquid immediately. No heat-transfer limitations are considered. The larger the difference in temperature between the vapor entering and the liquid leaving the column,

**Table 2. Acetone Absorber Specifications**

| | | |
|---|---|---|
| DECHEMA K model | | |
| NRTL activity coefficient | | |
| Antoine vapor pressure | | |
| Excess enthalpy | | |
| Top pressure 1.01325 (bar) | | |
| Estimated pressure drop | | |
| Feed stage | 1 | 30 |
| Pressure (atm) | 1.0 | 1.0 |
| Temperature (°C) | 24.9 | 25.0 |
| Component flows (mol/s) | | |
| Nitrogen | 0.0 | 10.0 |
| Acetone | 0.0 | 1.0 |
| Water | 40.0 | 0.0 |
| Section | | 1 |
| First stage | | 1 |
| Last stage | | 30 |
| Column diameter (m) | | 0.42 |
| Total tray area ($m^2$) | | 0.139 |
| Number of flow passes | | 1 |
| Tray spacing (m) | | 0.5 |
| Liquid flow path length (m) | | 0.301 |
| Active area (% total) | | 83.2 |
| Total hole area (% active) | | 24.3 |
| Downcomer area (% total) | | 8.4 |
| Hole diameter (m) | | 0.00476 |
| Hole pitch (m) | | 0.00907 |
| Weir length (m) | | 0.373 |
| Weir height (m) | | 0.0508 |
| Downcomer clearance (m) | | 0.0381 |
| Deck thickness (m) | | 0.00254 |

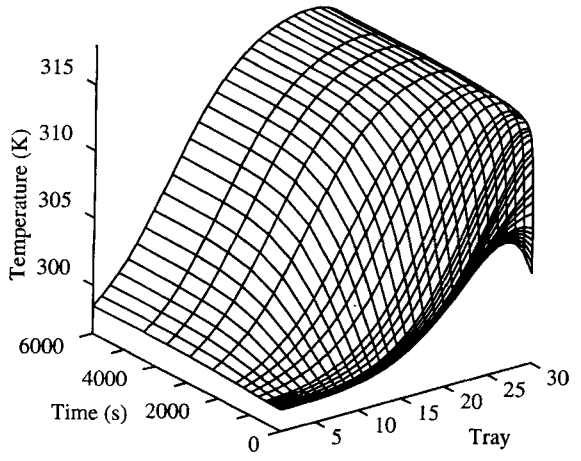


**Figure 8. Temperature profiles for the acetone absorber simulated with the nonequilibrium model.**

the less appropriate is the assumption of thermal equilibrium between phases.

Figure 10 shows the effects of the vapor temperature change for the concentration of acetone in the vapor leaving the column. Due to the lower temperatures in the column the change in acetone concentration is much less for the equilibrium model than that for the nonequilibrium model. Note that the response time is also different. Dynamic modeling of absorption columns like this can be important to ensure that environmental constraints are met at times even during short bursts in vapor flow, temperature, and contamination levels. This cannot be modeled with an equilibrium model if heat transfer plays an important role in the operation of the column. Furthermore, the nonequilibrium model has greater potential for modeling columns with trace components since mass-transfer effects have a large influence on the efficiency of the trace components.

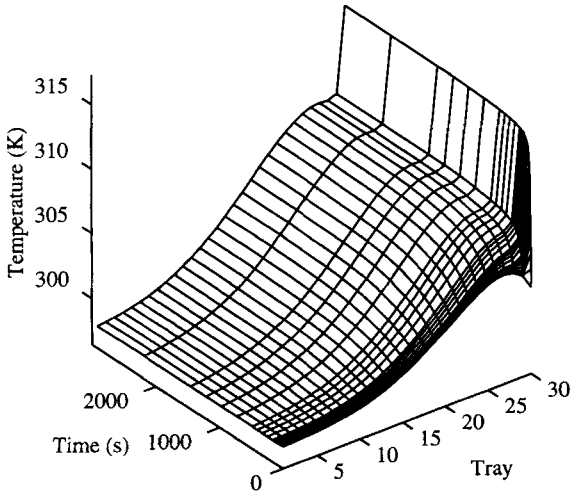


**Figure 9. Temperature profiles for the acetone absorber simulated with the equilibrium model.**

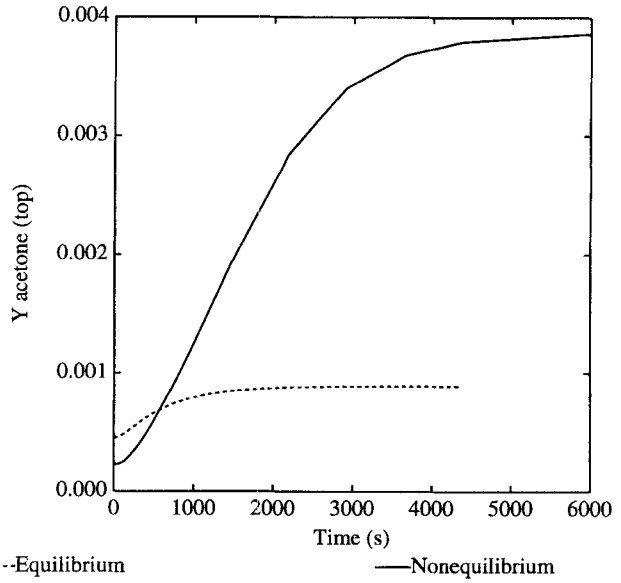


**Figure 10. Molefraction of acetone of absorber off-gas as a function of time for the equilibrium (----) and nonequilibrium (——) model.**

### *Debutanizer*

The third example is an industrial debutanizer taken from Gani et al. (1986); it is their only example where sufficient tray design details and steady-state information was supplied to allow simulation with a nonequilibrium model. The valve tray column is 1.67 m in diameter, and they used a constant efficiency for all trays. The efficiencies, backcalculated from a steady-state nonequilibrium simulation, vary from 0.62 to 0.67 for the rectifying section and range from 0.68 to 0.77 in the stripping section. This compares very well with the average tray column efficiency of 0.7 reported by Gani et al. The column was perturbed with a 5% increase in reflux rate, keeping the reboiler duty constant. The simulated bottoms pressure corresponds very well with that reported by Gani et al. (within 0.5 kPa). The results of the equilibrium and the nonequilibrium model are very similar in this case, as they should be.

### *Depropanizer*

The depropanizer column operates at a pressure of 15 bar, and illustrates the effects of the vapor holdups at high pressure. It shows that at these pressures the vapor holdups on and above the froth may be considerable and have to be properly modeled. Vapor holdup above the froth can be up to half as large as the combined liquid holdups on the tray and in the downcomer. Vapor holdup in the froth tends to be less then a tenth of the total liquid holdup and is less important. The downcomer liquid holdup varies with the size of the downcomer and can equal up to 50% of the liquid holdup on the tray. For this column the bottom flow rate is specified and the reflux ratio is increased from 2.5 to 4 at the start of the dynamic simulation. To check the effect of the inclusion of the vapor holdup above the froth, two nonequilibrium simulations have been run, one with all four of the holdups modeled separately and one with two holdups, but with the down-

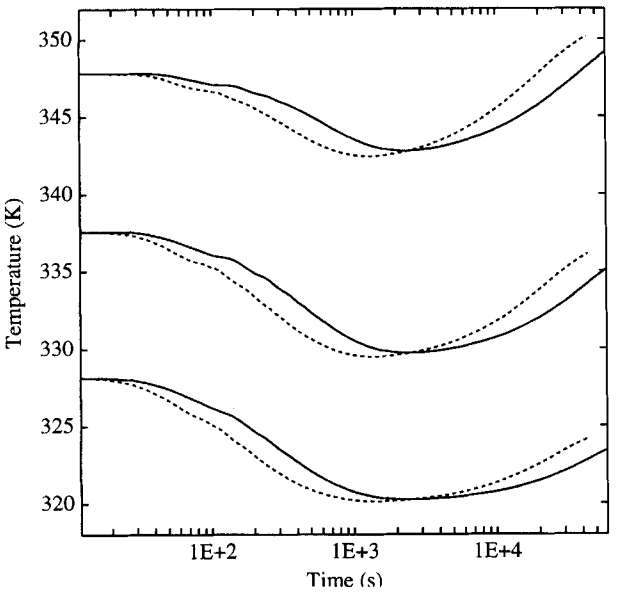


**Figure 11. Temperatures of trays 12, 15, and 18 in a depropanizer modeled by the nonequilibrium model with 2 holdups (----) and the 4 holdup model (——).**

comer liquid holdup lumped into one with the liquid holdup on the tray. The mass transfer is not influenced by this lumping (calculation of mass-transfer coefficients and interfacial area are computed independently of the holdup). Figure 11 shows the temperatures on three trays (12, 15, and 18) as a function of the time (the solid lines are for the four holdup models). Note the logarithmic time scale. It is apparent that the inclusion of the vapor holdup above the froth is significant as the transients converge more slowly toward the steady-state values (as they should with more total holdup in the column). Naturally, this has consequences for the time constants of the column and controller parameters derived from open-loop simulations.

## Conclusions

A rigorous nonequilibrium model has been developed where each phase in the froth and disengagement zone is considered as a separate, variable, completely mixed holdup and only mechanical equilibrium is assumed (equal pressure over the tray). Mass transfer occurs between the vapor and liquid in the dispersion on the tray. The nonequilibrium model includes tray sizing parameters and mass-transfer models and it is observed that these have a direct and significant influence on the column dynamics. Thus, the nonequilibrium model has the potential to include tray sizing parameters as part of the column design, control, and optimization. Without efficiencies the model is predictive; no estimates were needed to describe the performance of an existing industrial column, just tray design layout and specifications. Back-computed Murphree tray efficiencies are not constant over time, which implies that the equilibrium model should not be used for dynamic simulations. The difference between equilibrium and nonequilibrium simulation transients can be pronounced, both qualitatively and quantitatively. These differences are due to both mass- and heat-transfer limitations, which the equilibrium model ignores. There are significant differences in dynamic behavior of columns at higher pressures simulated with models that include or ignore the vapor holdup above the froth.

## Acknowledgments

This article is based on work supported by the National Science Foundation under grant CBT 88821005. Continuing support for this research is provided by BP International.

## Notation

$a$ = interfacial area, $m^2$
$A$ = area, $m^2$
$c$ = concentration, $kmol/m^3$
$h$ = heat-transfer coefficient, $W/m^2/K$
$K$ = equilibrium constant
$M$ = molecular weight, kg/kmol
$V$ = vapor flow rate, kmol/s; volume, $m^3$
$y$ = vapor mole fraction
$\phi$ = fugacity coefficient
$\gamma$ = activity coefficient
$\rho$ = density, $kg/m^3$

### *Superscripts and Subscripts*

$b$ = bottom; bubbling area plate
$c$ = cross-sectional area
$t$ = top
$\mu$ = from stage $\mu$

## Literature Cited

Boston, J. F., and H. B. Britt, "An Advanced System for the Simulation of Batch Distillation Operations," *Foundation of Computer-Aided Chemical Process Design*, R. S. H. Mah and W. D. Seider, eds., Engineering Foundation, New York (1981).

Bulirsch, R., and J. Stoer, "Numerical Treatment of Ordinary Differential Equations by Extrapolation Methods," *Num. Math.*, **8**, 1 (1966).

Cameron, I. T., C. A. Ruiz, and R. Gani, "A Generalized Model for Distillation Columns: II. Numerical and Computational Aspects," *Comp. Chem. Eng.*, **12**(5), 377 (1988).

Cuille, P. E., and G. V. Reklatis, "Dynamic Simulation of Multicomponent Batch Rectification with Chemical Reactions," *Comp. Chem. Eng.*, **10**(4), 389 (1986).

Distefano, G. P., "Mathematical Modeling and Numerical Integration of Multicomponent Batch Distillation Equations," *AIChE J.*, **14**, 190 (1968).

Duff, I. S., "A Set of FORTRAN Subroutines for Sparse Unsymmetric Linear Equations," AERE Harwell Report R8730, HMSO, London (1979).

Gani, R., C. A. Ruiz, and I. T. Cameron, "A Generalized Model for Distillation Columns: I. Model Description and Applications," *Comp. Chem. Eng.*, **10**(3), 181 (1986).

Gani, R., C. A. Ruiz, and I. T. Cameron, "Studies in the Dynamics of Startup and Shutdown Operations of Distillation Columns," *Proc. XVIII Congress: The Use of Computers in Chemical Engineering*, CEF 87, Giardini Naxos, Sicily, Italy (Apr. 26–30, 1987a).

Gani, R., and C. A. Ruiz, "Simulation of Startup and Shutdown Behavior of Distillation Operations," *Ind. Chem. Eng. Symp. Ser.*, No. 104, B39 (1987b).

Gani, R., and I. T. Cameron, "Extension of Dynamic Model of Distillation Columns to Steady-State Simulation," *Comp. Chem. Eng.*, **13**(3), 271 (1989).

Gear, C. W., *Numerical Initial Value Problems in Ordinary Differential Equations*, Prentice-Hall, Englewood Cliffs, N.J. (1971a).

Gear, C. W., "Simultaneous Numerical Solution of Differential-Algebraic Equations," *IEEE Trans. Circuit Theory*, **CT-18**, 89 (1971b).

Gerster, J. A., A. B. Hill, N. N. Hochgraf, and D. G. Robinson, *Tray Efficiencies in Distillation Columns*, AIChE, New York (1958).

Holl, P., W. Marquardt, and E. D. Gilles, "DIVA—A Powerful Tool for Dynamic Process Simulation," *Comp. Chem. Eng.*, **12**, 421 (1988).

Holland, C. D., and A. L. Liapis, *Computer Methods for Solving Dynamic Separation Problems*, McGraw-Hill, New York (1983).

Howard, G. M., "Unsteady-State Behavior of Multicomponent Distillation Columns," *AIChE J.*, **16**, 1023 (1970).

Huckaba, C. E., F. P. May, and F. R. Franke, "An Analysis of Transient Conditions in Continuous Distillation Operations," *Chem. Eng. Prog. Symp. Ser.*, **59**(46), 38 (1963).

Huckaba, C. E., F. R. Franke, F. P. May, B. T. Fairchild, and G. P. Distefano, "Experimental Confirmation of a Predictive Model for Dynamic Distillation," *Chem. Eng. Prog. Symp. Ser.*, **61**(55), 126 (1965).

Kooijman, H. A., and R. Taylor, "On the Estimation of Diffusion Coefficients in Multicomponent Liquid Systems," *Ind. Eng. Chem. Res.*, **30**(6), 1217 (1991).

Kooijman, H. A., "Dynamic Nonequilibrium Column Simulation," PhD Thesis, Clarkson Univ., Potsdam, New York (1995).

Krishnamurthy, R., and R. Taylor, "A Nonequilibrium Stage Model of Multicomponent Separation Processes. Part I: Model Description and Method of Solution," *AIChE J.*, **31**(3), 449 (1985a).

Krishnamurthy, R., and R. Taylor, "A Nonequilibrium Stage Model of Multicomponent Separation Processes: II. Comparison with Experiment," *AIChE J.*, **31**(3), 456 (1985b).

Krishnamurthy, R., and R. Taylor, "A Nonequilibrium Stage Model of Multicomponent Separation Processes: III. The Influence of Unequal Component Efficiencies in Process Design Problems," *AIChE J.*, **31**(12), 1973 (1985c).

Krishnamurthy, R., and R. Taylor, "Simulation of Packed Distillation and Absorption Columns," *Ind. Eng. Chem. Process Des. Dev.*, **24**, 513 (1985d).

Krishnamurthy, R., and R. Taylor, "Absorber Simulation and Design Using a Nonequilibrium Stage Model," *Can. J. Chem. Eng.*, **64**, 1976 (1986).

Lao, M., J. P. Kingsley, R. Krishnamurthy, and R. Taylor, "A Nonequilibrium Stage Model of Multicomponent Separation Processes. Part VI: Simulation of Liquid-Liquid Extraction," *Chem. Eng. Commun.*, **86**, 73 (1989).

Luyben, W. L., V. S. Verneuil, Jr., and J. A. Gerster, "Experimental Transient Response of a Pilot-Plant Distillation Column: IV. Response of a Ten-Tray Column," *AIChE J.*, **10**, 357 (1964).

Mah, R. S., S. Michaelsen, and R. W. H. Sargent, "Dynamic Behavior of Multicomponent Multistage System," *Chem. Eng. Sci.*, **17**, 619 (1962).

Michelsen, M. L., "An Efficient General Purpose Method of Integration of Stiff Ordinary Differential Equations," *AIChE J.*, **22**(3), 544 (1976).

Pantelides, C. C., "SPEEDUP—Recent Advances in Process Simulation," *Comp. Chem. Eng.*, **12**, 745 (1988).

Pantelides, C. C., D. Gritsis, K. R. Morrison, and R. W. H. Sargent, "The Mathematical Modeling of Transient Systems Using Differential-Algebraic Equations," *Comp. Chem. Eng.*, **12**(5), 449 (1988).

Powers, M. F., D. J. Vickery, A. Arehole, and R. Taylor, "A Nonequilibrium Stage Model of Multicomponent Separation Processes: V. Computational Methods for Solving the Model Equations," *Comp. Chem. Eng.*, **12**(12), 1229 (1988).

Prokopakis, G. J., and W. D. Seider, "Dynamic Simulation of Azeotropic Distillation Towers," *AIChE J.*, **29**(6), 1017 (1983).

Ranzi, E., M. Rovaglio, T. Faravelli, and G. Biardi, "Role of Energy Balances in Dynamic Simulation of Multicomponent Distillation Columns," *Comp. Chem. Eng.*, **12**(8), 783 (1988).

Ruiz, C. A., I. T. Cameron, and R. Gani, "A Generalized Model for Distillation Columns: III. Study of Startup Operations," *Comp. Chem. Eng.*, **12**(1) 1 (1988).

Sherman, A. H., "NSPIV, a FORTRAN Subroutine for Sparse Gaussian Elimination with Partial Pivoting," *ACM Trans. Math. Software*, **4**, 391 (1978).

Sivasubramanian, M. S., R. Taylor, and R. Krishnamurthy, "A Nonequilibrium Stage Model of Multicomponent Separation Processes: IV. A Novel Approach to Packed Column Design," *AIChE J.*, **33**(2), 325 (1987).

Taylor, R., and H. A. Kooijman, "Composition Derivatives of Activity Models (for the Estimation of Thermodynamic Factors in Diffusion)," *Chem. Eng. Comm.*, **102**, 87 (1991).

Taylor, R., H. A. Kooijman, and M. R. Woodman, "Industrial Applications of a Nonequilibrium Model of Distillation and Absorption Operations," *Ind. Chem. Eng. Symp. Ser.*, No. 128, Birmingham, UK, A415 (1992).

Taylor, R., and R. Krishna, *Multicomponent Mass Transfer*, Wiley, New York (1993).

Taylor, R., H. A. Kooijman, and J.-S. Hung, "A Second Generation Nonequilibrium Model for Computer Simulation of Multicomponent Separation Processes," *Comp. Chem. Eng.*, **18**(3), 205 (1994).

Waggoner, R. C., and C. D. Holland, "Solution of Problems Involving Conventional and Complex Distillation Columns at Unsteady-State Operation," *AIChE J.*, **11**, 112 (1965).

*Manuscript received Apr. 21, 1994, and revision received Sept. 26, 1994.*